Additional computational details

Singlet/singlet conical intersections ($S_3(\pi\pi^*_{CC})/S_2(\pi\pi^*_{CS})$), ($S_2(\pi\pi^*_{CC})/S_1(n\pi^*_{CS})$) and ($S_1(\pi\pi^*_{CC})/S_0$) and singlet/triplet minimum energy crossing points ($T_1(\pi\pi^*_{CS})_1/S_0$), ($T_1(n\pi^*_{CS})/S_0$), and ($T_1(\pi\pi^*_{CS})_2/S_0$), were optimized at CASSCF[1](12,10)/ANO-S[2] level of theory. This active space comprises 12 electrons distributed in 10 orbitals, and includes a lone pair of the S atom, 5π and 4π* orbitals. For further details on the active space composition and the basis set contractions used, see Ref. 3. The different topology of the CASPT2 and CASSCF potential energy surfaces usually translates in the displacement of the degeneracy points to nearby regions. In these cases, the geometries of the CASSCF degeneracy points were slightly modified until an energy difference smaller than 0.09 eV between the two intersecting states was reached at MS-CASPT2[4,5] level of theory.

The probability of intersystem crossing from the triplet manifold to the ground state was estimated by computing spin-orbit coupling terms at the singlet/triplet minimum energy crossing points. These calculations were performed using SA-CASSCF(12,10)/ANO-RCC[6] (contracted as C,N [3s2p1d]/S[4s3p1d]/H[2s1p]) wavefunctions including five singlet and five triplet states.

In order to provide further insight into the global deactivation mechanism, Linear Interpolated calculations in Cartesian Coordinates (LICC) were performed (Figures S1-S3) at CASSCF(12,10)/ANO-S level of theory over 5 singlet roots. Minimum energy paths (MEPs) in Figures S4-S9 were computed following the intrinsic reaction coordinate (IRC)[7] algorithm to connect each conical intersection with the corresponding stationary points. These calculations were performed using the CASSCF/ANO-S protocol with the (12,10) active space and 5 singlet roots.

Final energies were refined with a larger active space (14,12) and the basis set ANO-L[8] as described in ref 3. However, within the present work the number of roots was increased up to 5 (3 roots were considered in our previous work, Ref 3) in order to include high-lying excited states involved in the new deactivation mechanism, see Table S1. A real level shift parameter of 0.3 au was added to the zero order Hamiltonian to prevent the appearance of intruder states.[9]

All the calculations were performed with the 7.4 version of MOLCAS program.[10]

Reparameterization of the semiempirical Hamiltonian

We applied a semiempirical configuration interaction approach using molecular orbitals obtained from a SCF calculation with floating occupation numbers (FOMO-CI)[11,12]. The CI space was of CAS type with four electrons in four orbitals. In particular, the active orbitals were the n lone pair, one π and two π* (π^*_{CS} and π^*_{CC}). The gaussian width used in the FOMO procedure was w = 0.1 a.u. The energies and geometries of the stationary points and conical intersections playing a role in the deactivation mechanism of 6-TG[3] were used to reparameterize the semiempirical AM1 hamiltonian, by minimizing the function:

$$F(P) = \sum_i \left(\frac{V_i^{(T)} - V_i^{(S)}(P)}{V_i^{(T)}} \right)^2 W_i$$

Here P is the set of semiempirical parameters, $V_i^{(T)}$ is a target quantity, $V_i^{(S)}$ the corresponding semiempirical value obtained with the FOMO-CI procedure and the Wi are positive weights. The search of the minimum of F(P) was carried out by coupling a simulated annealing procedure with the simplex method, as described in Cusati et al ref. 12. The target values used in the reparameterization procedure, together with the corresponding final semiempirical results, are shown in Tables S_3 and S_4. As it is evident from the values of the dihedral angle θ=$SC_9C_3C_4$, at the S_1, T_1 and T_2 equilibrium geometries the sulphur atom lies out of the plane of the purine skeleton. To reproduce this feature we added to the semiempirical Hamiltonian a potential term:

$$U(\theta, \phi) = [-P_1(cos\theta + 1) + P_2(cos^2\theta - 1)]cos\phi$$

where ϕ is the dihedral angle C9N8C7N6 and P1, P2 are numerical parameters that have been determined by minimizing the F(P) function. The full set of semiempirical parameters obtained,together with the values of P_1 and P_2, are provided in this supporting information.

As one can see from Table S3, the reparameterized semiempirical FOMO-CI calculations underestimate the vertical transition energies at the ground state equilibrium geometry by 0.5 eV, with the exception of the T_3 state. The energy ordering of the singlet and triplet states is correct: the inclusion of the oscillator strengths in the reparameterization procedure was instrumental in characterizing the n → π* and π → π* excitations. At the FOMO-CI level, theT_3 vertical excitation energy is close to those of T_1 and T_2 and 1.4 eV lower than the ab initio result. The T_3 state was therefore included in the surface hopping simulations, but does not play a relevant role in the dynamics. At the ground state geometry S_1 and S_2 have, respectively, $n\pi^*_{CS}$ and $\pi\pi^*_{CS}$ character; as the S atom lies roughly in the plane of the two rings, the S_0-S_1 oscillator strength is almost zero, while the S_2 state is bright. At its equilibrium geometry the S_2 state is very close in energy to S_1; this feature is very important in the photorelaxation dynamics and is correctly reproduced at semiempirical level (see Table S3). The low energy ($S_1(\pi\pi^*_{CC})/S_0$) conical intersection (involving the high lying S_3 state at FC geometry, not initially considered in the first quantum calculations study of the deactivation mechanism of 6-TG, see Figure 4)was first discovered at semiempirical level and subsequently confirmed by ab initio calculations and inserted among the final reparameterization targets. This conical intersection and the higher energy ($S_1(\pi\pi^*_{CS})/S_0$) crossing referred in Tables S3-S4 appear to be not too accurately reproduced at semiempirical level (i.e. 0.93 and 0.44 eV below the ab initio findings, respectively); however, they turn out to play a minor role in the dynamics.

Thanks also to the introduction of the potental term $U(\theta, \phi)$ referred above, the geometrical parameters shown in Table S4 are well reproduced by the

semiempirical calculations, with the exception of the C-S bond length, that is systematically underestimated.

For the evaluation of the SOC we used the one-electron effective spin-orbit Hamiltonian defined by Böckmann et al[13,14]. The associated semiempirical atomic parameters $\xi_{\alpha,p}$ were obtained, for α=C and N, from the corresponding atomic terms[15], as shown in ref. 13 ($\xi_{C,p}$= 24.6 and $\xi_{N,p}$= 4 cm^{-1}). For sulphur $\xi_{S,p}$ was adjusted in order to reproduce the ab initio data for (S1(nπ*CS)/T1(ππ*CS)) SOC at the S1(nπ*CS)min geometry (164 cm−1). We obtained $\xi_{S,p}$ = 500cm^{-1}, which is of the same order of magnitude of the value (384 cm^{-1}) one would extract from the ground state splitting of atomic sulphur.

1 B. O. Roos, in *Ab initio Methods in Quantum Chemistry II,* ed. K. P. Lawley, Wiley, Chichester, 1987.
2 K. Pierloot, B. Dumez, P.-O Widmark, B. O. Roos, Theor Chim Acta 1995, **90**, 87.
3 L. Martínez-Fernández, L. González and I. Corral, *Chem. Commun*. 2012, **48**, 2134.
4 K. Andersson, P. Å. Malmqvist and B. O. Roos, *J. Chem. Phys.*, 1992, **96**, 1218.
5 J. Finley, P. Å. Malmqvist, B. O. Roos and L. Serrano-Andrés, *Chem. Phys. Lett.*, 1998, **288**, 299.
6 B. O. Roos, V. Veryazov, and P.-O. Widmark. *Theor. Chim. Acta*, 2004, **111**, 345.
7 A. Migani and M. Olivucci, in *Conical Intersections: Electronic Structure, Dynamics and Spectroscopy, Vol. 15,* ed. W. Domcke, D. Yarkony, H. Köppel, World Scientific, Singapore, 2004.
8 P.-O Widmark, P.-A. Malmqvist, B. O. Roos, Theor Chim Acta 1990, **77**, 291.
9 B. O. Roos and K. Andersson, *Chem. Phys. Lett.*, 1995, **245**, 215.
10 F. Aquilante, L. De Vico, N. Ferré, G. Ghigo, P. Å. Malmqvist, P. Neogrády, T. B. Pedersen, M. Pitoňák, M. Reiher, B. O. Roos, L. Serrano-Andrés, M. Urban, V. Veryazov and R. Lindh, *J. Comput. Chem.,* 2010, **31**, 224.
11 G. Granucci, A. Toniolo and M. Persico, *J. Chem. Phys.*, 2001, **114**, 10608.
12 T. Cusati, G. Granucci, E. Martínez-Nuñez, F. Martini, M. Persico and S. Vázquez, *J. Phys. Chem. A*, 2012, **116**, 98.
13 G. Granucci and M. Persico, *J. Comput. Chem.*, 2011, **32**, 2690.
14 M. Böckmann, M. Klessinger and M. C. Zerner, *J. Phys. Chem.*, 1996, **100**, 10570.
15 For C the ground state term 3P was considered, while for N, which has a 4So ground state, we took the first excited term 2Do. See Y. Ralchenko, A. Kramida, J. Reader and NIST ASD Team, NIST Atomic Spectra Database (2011). National Institute of Standards and Technology, Gaithersburg, MD.

Figure S1. CASSCF Linear Interpolation in Cartesian Coordinates connecting the FC region with the ($S_1(\pi\pi^*_{CC})/S_0$) conical intersection.

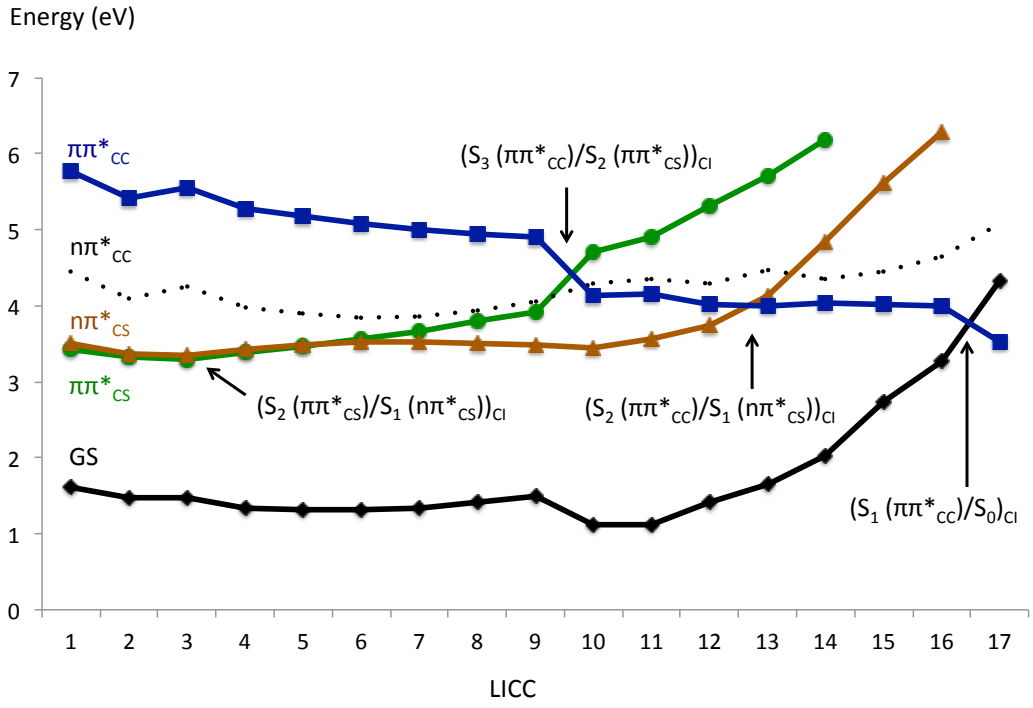

Figure S2. CASSCF Linear Interpolation in Cartesian Coordinates connecting the $n\pi^*_{CS}$ minimum with the ($S_1(\pi\pi^*_{CC})/S_0$) conical intersection.

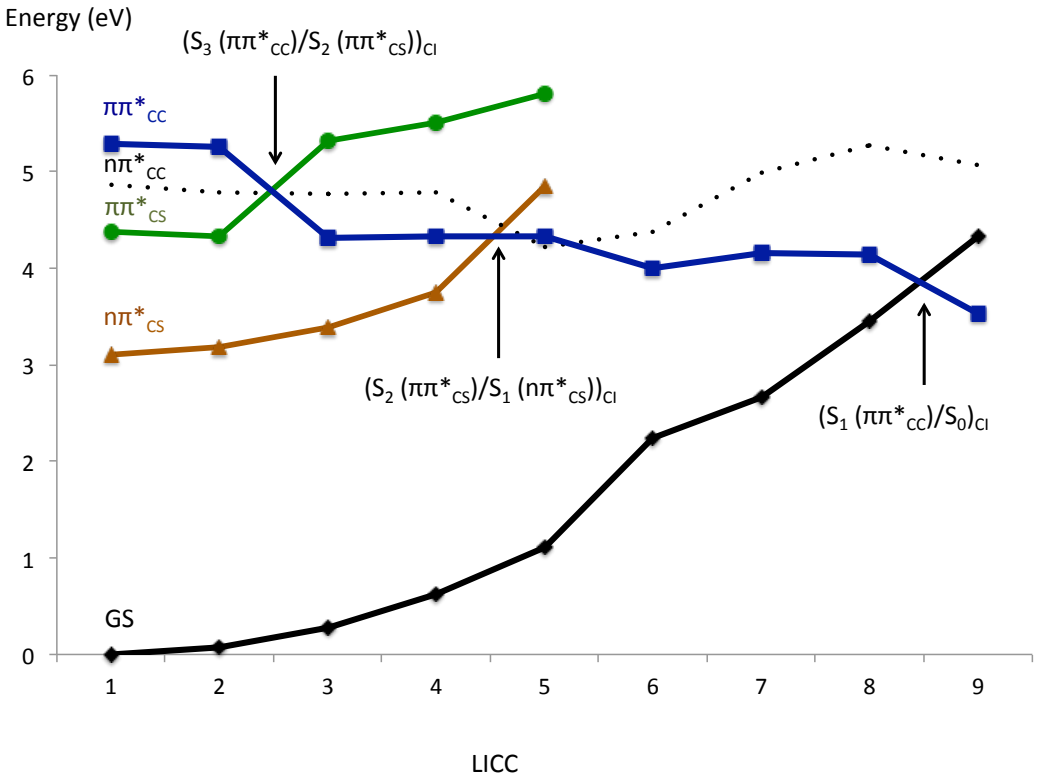

Figure S3. CASSCF Linear Interpolation in Cartesian Coordinates connecting the $\pi\pi^*_{CS}$ minimum with the $(S_1(\pi\pi^*_{CC})/S_0)$ conical intersection.

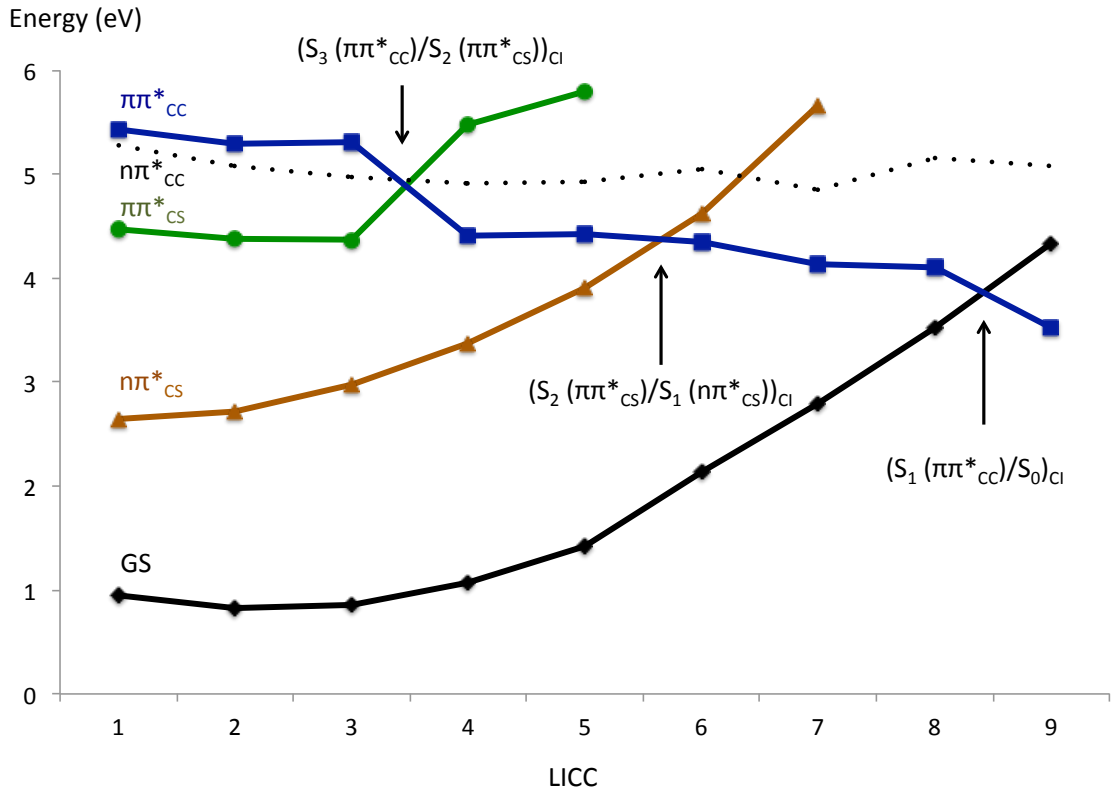

Figure S4. CASSCF Minimum energy paths from the $(S_1(\pi\pi^*_{CC})/S_0)$ conical intersection following the S_0 and S_1 gradients.

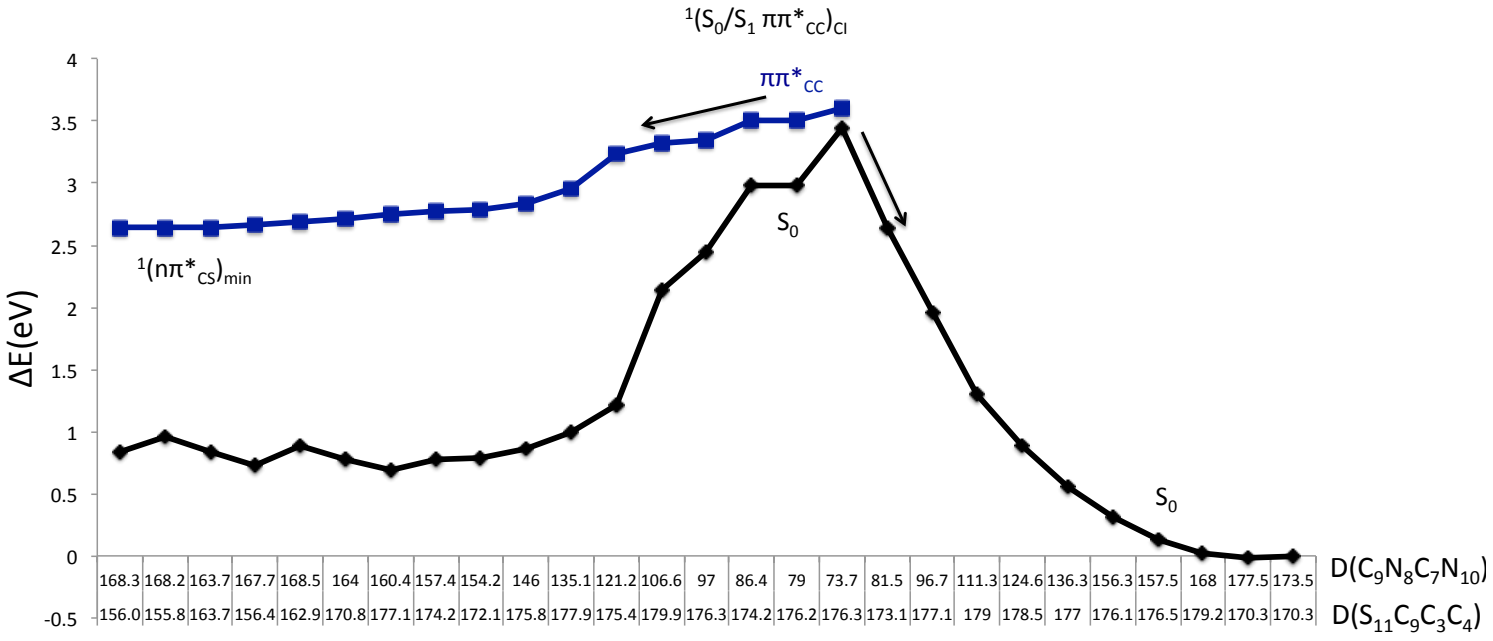

Figure S5. CASSCF Minimum energy paths from the ($S_3(\pi\pi^*_{CC})/S_2(\pi\pi^*_{CS})$) conical intersection following the S_2 gradient.

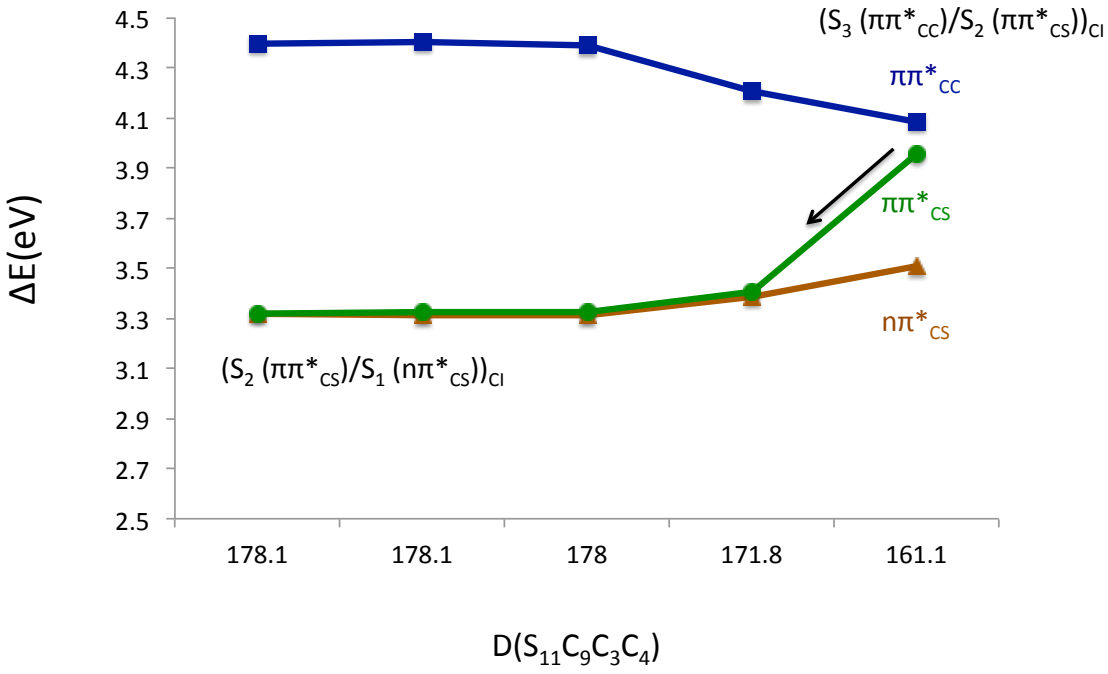

Figure S6. CASSCF Minimum energy paths from the ($S_2(\pi\pi^*_{CC})/S_1(n\pi^*_{CS})$) conical intersection following the S_1 gradient.

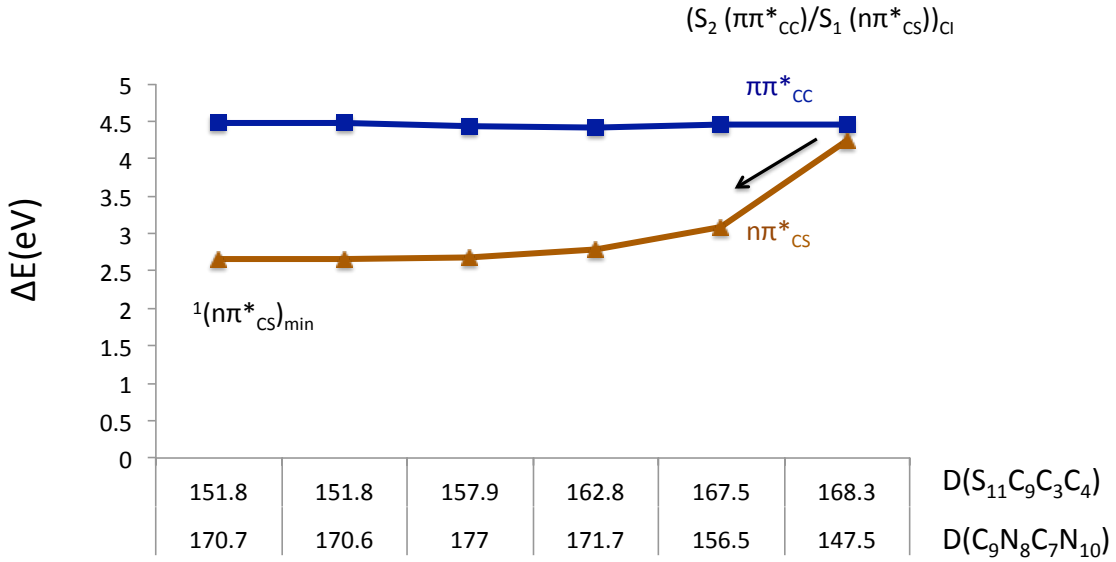

Figure S7. CASSCF Minimum energy paths starting from $(T_1(\pi\pi^*_{CS})_1/S_0)_{CI}$.

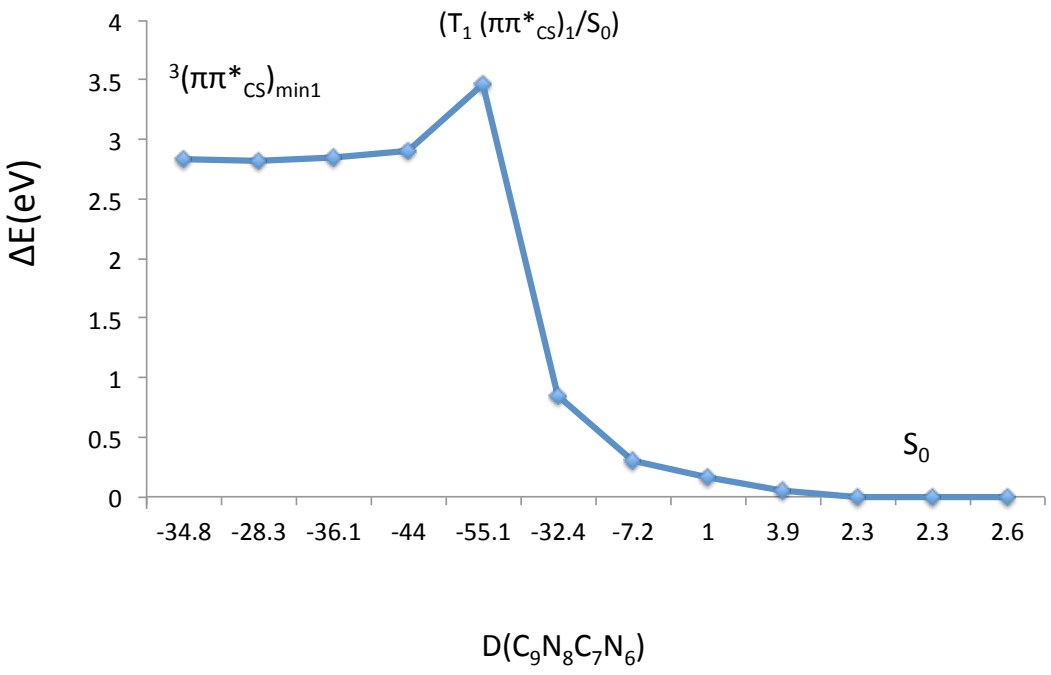

Figure S8. CASSCF Minimum energy paths starting from $(T_1(\pi\pi^*_{CS})_2/S_0)_{CI}$.

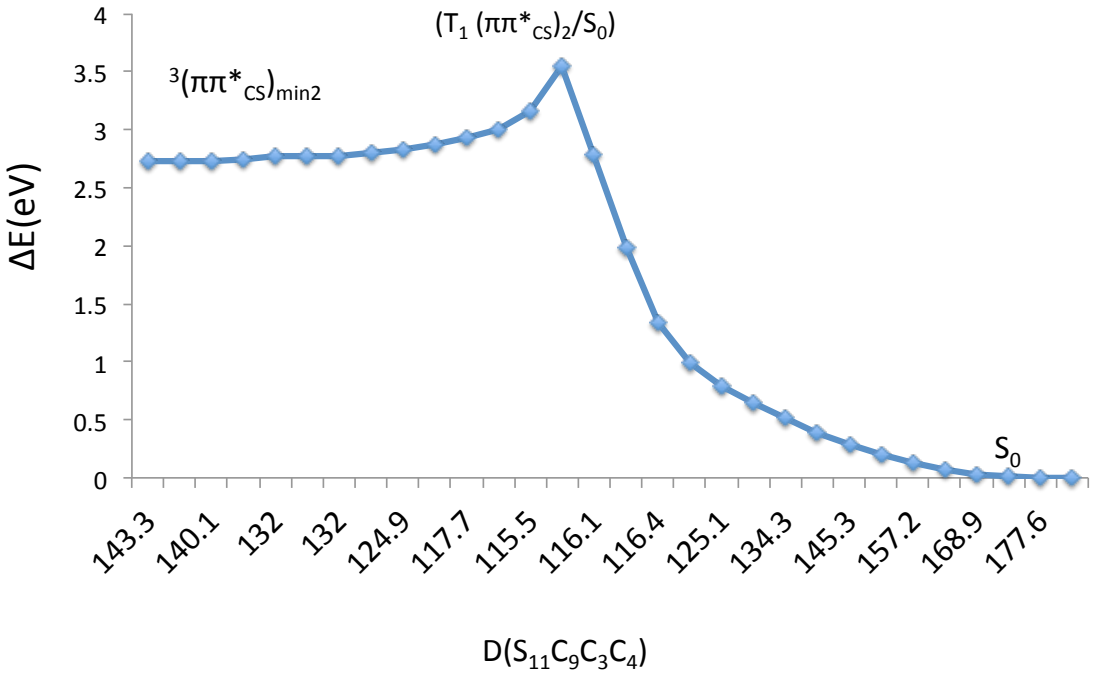

Figure S9. CASSCF Minimum energy paths from $(T_1(n\pi^*_{CS})/S_0)_{CI}$.

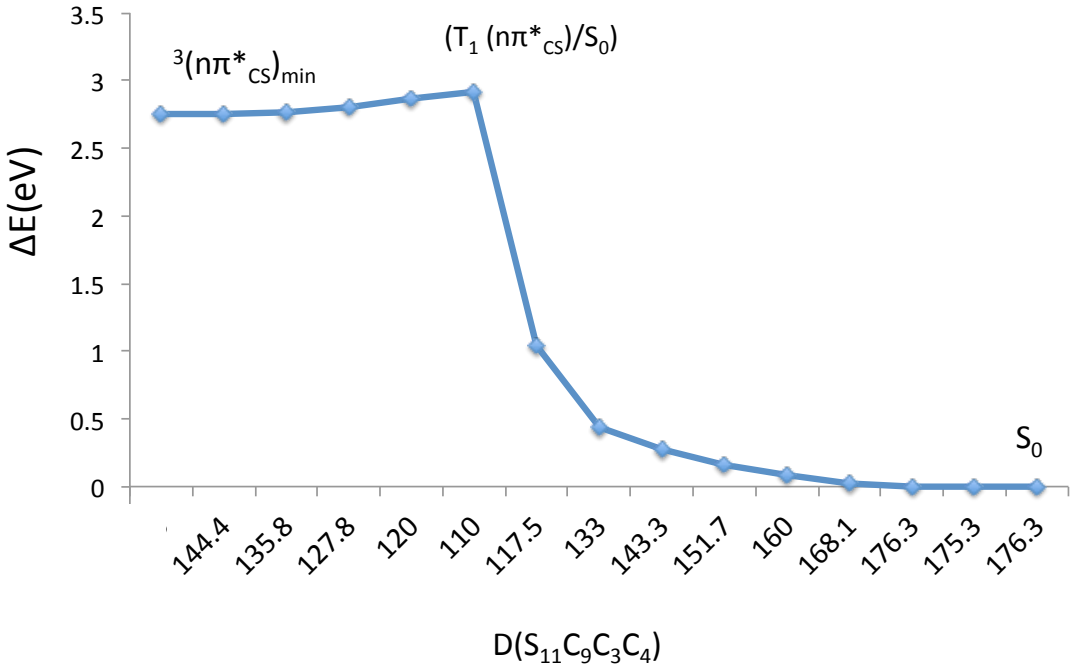

Figure S10. Representative distances in angstroms and dihedral angles in degrees for the CASSCF optimized structures of the conical intersections.

$(S_3\ (\pi\pi^*_{CC})/S_2\ (\pi\pi^*_{CS}))_{CI}$

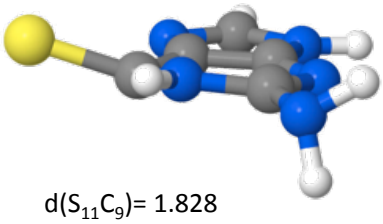

$d(S_{11}C_9)$= 1.828
$D(S_{11}C_9C_3C_4)$= 161.1
$D(C_9N_8C_7N_{10})$=-164.6

$(S_2\ (\pi\pi^*_{CC})/S_1\ (n\pi^*_{CS}))_{CI}$

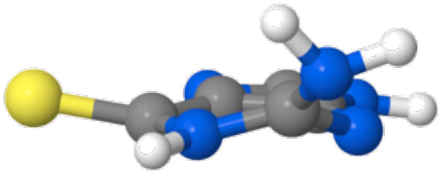

$d(S_{11}C_9)$= 1.699
$D(S_{11}C_9C_3C_4)$= 168.3
$D(C_9N_8C_7N_{10})$=147.5

$(S_1\ (\pi\pi^*_{CC})/S_0)_{CI}$

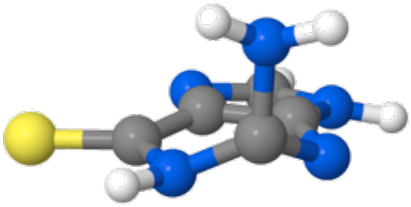

$d(S_{11}C_9)$= 1.647
$D(S_{11}C_9C_3C_4)$= -176.2
$D(C_9N_8C_7N_{10})$=73.7

$(T_1\ (\pi\pi^*_{CS})_2/S_0)$

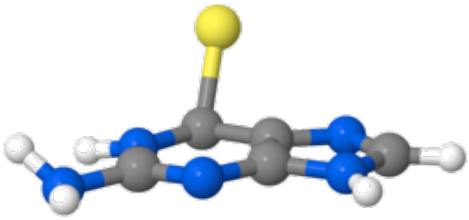

$d(S_{11}C_9)$= 1.858
$D(S_{11}C_9C_3C_4)$= 117.1
$D(C_9N_8C_7N_6)$= -1.9

$(T_1\ (n\pi^*_{CS})/S_0)$

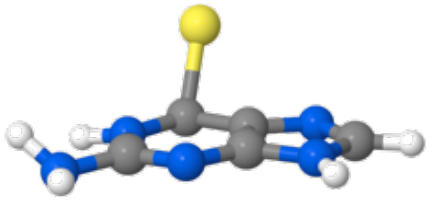

$d(S_{11}C_9)$= 1.858
$D(S_{11}C_9C_3C_4)$= 117.1
$D(C_9N_8C_7N_6)$=2.8

$(T_1\ (\pi\pi^*_{CS})_1/S_0)$

$d(S_{11}C_9)$= 1.798
$D(S_{11}C_9C_3C_4)$= -158.3
$D(C_9N_8C_7N_6)$=-64.1

Figure S11. Time evolution of a representative trajectory from the singlet only dynamics evolving on the S_1 potential until the final time of the simulation. Red, green and blue curves correspond to the S_0, S_1 and S_2 potentials. Black dots show the potential visited by the system at a specific time. Snapshots at relevant times along the trajectory are also presented.

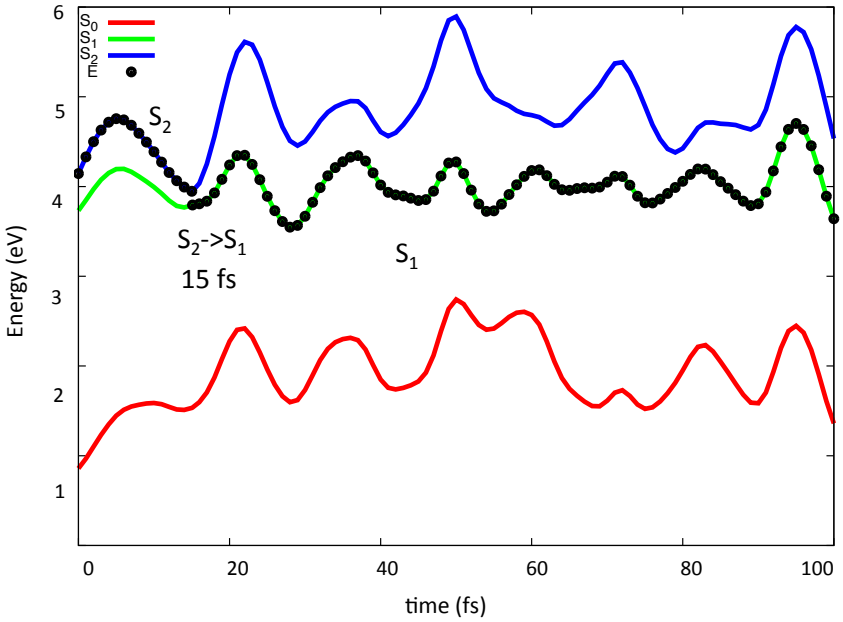

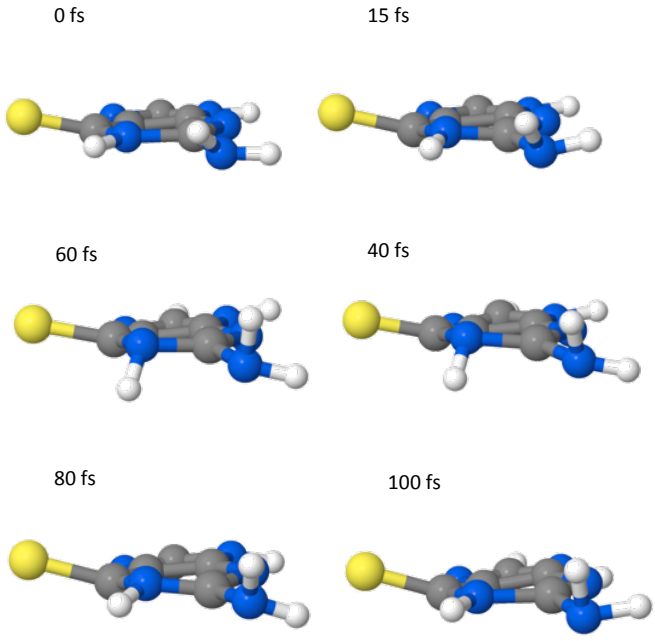

Figure S12. Selected parts, (0-100fs) (a) and (5500-5700fs) (b), of a representative trajectory decaying to the S_0. Red, green and blue curves correspond to the S_0, S_1 and S_2 potentials. Black dots show the potential visited by the system at a specific time. Snapshots at relevant times along the trajectory are also presented.

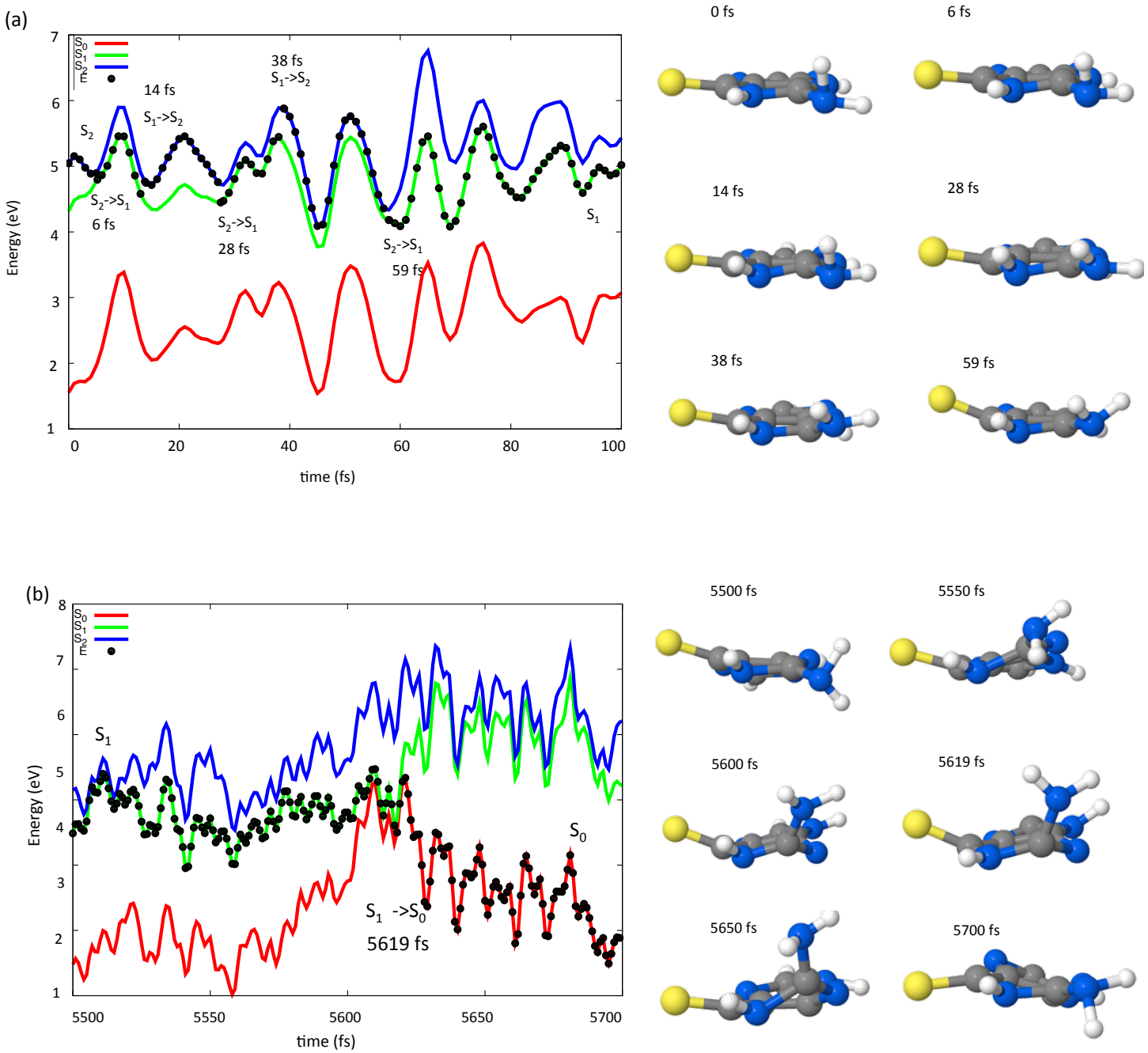

Table S1. MS-CASPT2//CASSCF(14,12)/ANO-L energies (in eV) for the lowest lying singlet and triplet states at the stationary points collected in Figures 2,3 and 4.

Structure	State	ΔE [eV]	Structure	State	ΔE [eV]
$^1(n_S\pi^*_{CS})_{min}$	GS	0.94	$^3(n_S\pi^*_{CS})_{min}$	$^3(\pi\pi^*_{CS})$	3.00
	$^1(n\pi^*_{CS})$	3.18		$^3(n\pi^*_{CS})$	3.09
	$^1(\pi\pi^*_{CS})$	4.01		$^3(\pi\pi^*_{CC})$	4.98
	$^1(\pi\pi^*_{CC})$	5.47		$^3(\pi\pi^*_{CC})$	5.65
	$^1(n\pi^*_{CC})$	5.55		$^3(n\pi^*_{CC})$	5.67
$^1(\pi\pi^*_{CS})_{min}$	GS	1.41	$^3(\pi\pi^*_{CS})_{TS}$	$^3(\pi\pi^*_{CS})$	3.55
	$^1(n\pi^*_{CS})$	3.91		$^3(n\pi^*_{CS})$	4.36
	$^1(\pi\pi^*_{CS})$	3.78		$^3(\pi\pi^*_{CC})$	4.72
	$^1(\pi\pi^*_{CC})$	5.10		$^3(\pi\pi^*_{CC})$	5.64
	$^1(n\pi^*_{CC})$	4.47		$^3(n\pi^*_{CC})$	4.87
$(S_2(\pi\pi^*_{CC})/S_1(n\pi^*_{CS}))_{CI}$	GS	1.50	$^3(\pi\pi^*_{CS})_{min1}$	$^3(\pi\pi^*_{CS})$	3.37
	$^1(n\pi^*_{CS})$	3.96		$^3(n\pi^*_{CS})$	4.12
	$^1(\pi\pi^*_{CS})$	3.85		$^3(\pi\pi^*_{CC})$	4.47
	$^1(\pi\pi^*_{CC})$	5.10		$^3(\pi\pi^*_{CC})$	5.38
	$^1(n\pi^*_{CC})$	4.51		$^3(n\pi^*_{CC})$	4.64
$(S_1(\pi\pi^*_{CS})/S_0)_{CI}$	GS	3.71	$^3(\pi\pi^*_{CS})_{min2}$	$^3(\pi\pi^*_{CS})$	3.00
	$^1(n\pi^*_{CS})$	5.41		$^3(n\pi^*_{CS})$	3.09
	$^1(\pi\pi^*_{CS})$	3.82		$^3(\pi\pi^*_{CC})$	4.98
	---			$^3(\pi\pi^*_{CC})$	5.65
	---			$^3(n\pi^*_{CC})$	5.67
$(S_1(n\pi^*_{CS})/S_0)_{CI}$	GS	4.51	$(T_1(\pi\pi^*_{CS})_1/S_0)_{CI}$	GS	4.41
	$^1(n\pi^*_{CS})$	4.87		$^3(\pi\pi^*_{CS})$	4.58
	$^1(\pi\pi^*_{CS})$	5.60		$^3(n\pi^*_{CS})$	5.05
	---			$^3(\pi\pi^*_{CC})$	6.51
	---			$^3(\pi\pi^*_{CC})$	7.56
$(S_3(\pi\pi^*_{CC})/S_2(\pi\pi^*_{CS}))_{CI}$	GS	1.17	$(T_1(\pi\pi^*_{CS})_2/S_0)_{CI}$	GS	3.08
	$^1(n\pi^*_{CS})$	3.73		$^3(\pi\pi^*_{CS})$	3.16
	$^1(\pi\pi^*_{CS})$	4.24		$^3(n\pi^*_{CS})$	3.81
	$^1(\pi\pi^*_{CC})$	4.33		$^3(\pi\pi^*_{CC})$	6.37
	$^1(\pi\pi^*_{CC})$	4.49		$^3(\pi\pi^*_{CC})$	5.77
$(S_3(\pi\pi^*_{CC})/S_2(\pi\pi^*_{CS}))_{CI}$	GS	1.37	$(T_1(n\pi^*_{CS})/S_0)_{CI}$	GS	3.50
	$^1(n\pi^*_{CS})$	4.38		$^3(\pi\pi^*_{CS})$	3.41
	$^1(\pi\pi^*_{CS})$	4.81		$^3(n\pi^*_{CS})$	3.98
	$^1(\pi\pi^*_{CC})$	4.33		$^3(\pi\pi^*_{CC})$	6.41
	$^1(\pi\pi^*_{CC})$	5.05		$^3(n\pi^*_{CC})$	6.77
$(S_1(\pi\pi^*_{CC})/S_0)_{CI}$	GS	4.00			
	$^1(\pi\pi^*_{CC})$	3.90			

Table S2. Cartesian coordinates (in Å) of the CASSCF optimized conical intersection structures.

Atom	X	Y	Z
	$(S_3(\pi\pi^*_{CC})/S_2(\pi\pi^*_{CS}))_{CI}$		
H	-2.464655	0.624347	-0.446557
H	-2.816632	-1.824332	-2.137345
H	-2.925939	-2.627698	-0.710052
H	2.191151	-2.613458	-0.000038
H	3.693878	-0.613573	0.650954
C	-1.564921	-1.190996	-0.691783
C	-0.444446	0.952379	-0.312980
C	0.701612	0.220642	-0.037785
C	0.618960	-1.215124	-0.225422
C	2.645096	-0.535063	0.372751
N	-1.556823	0.179182	-0.449098
N	-2.795662	-1.708716	-1.124277
N	-0.410111	-1.936435	-0.597666
N	1.984656	0.588832	0.315417
N	1.892085	-1.658813	0.043889
S	-0.624367	2.641551	0.362256

Atom	X	Y	Z
	$S_2(\pi\pi^*_{CC})/S_1(n\pi^*_{CS}))$		
H	2.406467	0.655842	-0.692046
H	0.800931	3.565257	0.611008
H	2.153164	2.653323	0.925956
H	-3.266796	0.987333	-0.114064
H	-3.569278	-1.518777	0.250162
C	0.727951	1.709153	-0.146851
C	0.873385	-0.696362	-0.237181
C	-0.534463	-0.612608	0.019383
C	-1.193604	0.652770	-0.076811
C	-2.621206	-1.037765	0.156259
N	1.436763	0.606282	-0.468973
N	1.408159	2.839796	0.280815
N	-0.648673	1.785942	-0.441993
N	-1.472234	-1.632530	0.187264
N	-2.512339	0.341490	0.001890
S	1.869793	-2.032108	0.094347

Atom	X	Y	Z
	$(S_1(\pi\pi^*_{CC})/S_0)_{CI}$		
H	-2.350420	0.870050	-1.021890
H	-2.980440	-0.887650	0.988480
H	-2.452510	-2.438700	0.706540
H	2.249260	-2.601070	-0.264930
H	3.642200	-0.668560	0.746280
C	-1.627410	-1.090130	-0.590630
C	-0.470440	1.001250	-0.232350
C	0.604380	0.132520	0.168290
C	0.578440	-1.269010	-0.217300
C	2.567300	-0.606200	0.494890
N	-1.507190	0.298330	-0.890060
N	-2.170480	-1.458600	0.697190
N	-0.381550	-1.828800	-0.918400
N	1.851170	0.514300	0.629690
N	1.865920	-1.703510	0.020990
S	-0.556460	2.623330	0.042280

Atom	X	Y	Z
	$(T_1(\pi\pi^*_{CS})_1/S_0)_{CI}$		
H	-2.320750	0.799413	-0.505446
H	-2.949494	-2.130847	-0.320956
H	-3.222823	-1.848719	1.248362
H	2.240308	-2.516605	-0.236499
H	3.808875	-0.571510	0.045372
C	-1.662087	-0.856403	0.509238
C	-0.314110	0.981902	-0.073397
C	0.752149	0.274502	0.325562
C	0.618848	-1.200278	0.077309
C	2.742333	-0.470617	0.083942
N	-1.503145	0.307742	-0.254565
N	-2.950123	-1.413511	0.385458
N	-0.457144	-1.828102	-0.080294
N	2.131252	0.620095	0.345725
N	1.928749	-1.574123	-0.181414
S	-0.307761	2.740254	-0.449320

Atom	X	Y	Z
	$(T_1(\pi\pi^*_{CS})_2/S_0)_{CI}$		
H	-2.416465	0.633844	-0.616533
H	-2.702905	-2.629950	0.303641
H	-3.491236	-1.181624	0.435760
H	2.197274	-2.445908	0.323709
H	3.829955	-0.543513	-0.118532
C	-1.530680	-1.068471	-0.026311
C	-0.407582	1.106779	-0.431623
C	0.780342	0.313973	-0.223922
C	0.669825	-1.036259	0.067718
C	2.765782	-0.438806	-0.118388
N	-1.541612	0.248252	-0.340034
N	-2.763207	-1.688706	-0.022177
N	-0.465783	-1.767744	0.208999
N	2.118914	0.658752	-0.342309
N	1.934124	-1.505860	0.134593
S	-0.114976	2.232675	1.017119

Atom	X	Y	Z
	$(T_1(n\pi^*_{CS})/S_0)_{CI}$		
H	-2.321558	0.674114	-0.654902
H	-2.747496	-2.575509	0.264344
H	-3.407095	-1.110529	0.634016
H	2.233224	-2.513201	0.239795
H	3.883953	-0.610924	-0.071374
C	-1.499936	-1.059671	0.003288
C	-0.322857	1.095666	-0.422720
C	0.853678	0.271719	-0.231441
C	0.716358	-1.066871	-0.011432
C	2.820282	-0.502412	-0.095755
N	-1.489908	0.314224	-0.235529
N	-2.773481	-1.603231	0.037394
N	-0.455271	-1.780548	0.134329
N	2.182785	0.616336	-0.283593
N	1.981542	-1.566817	0.071736
S	-0.810735	2.321681	0.908059

Table S3. Reparameterization of the AM1 Hamiltonian: target values for energy (eV) and oscillator strength data, and corresponding semiempirical results. Conical intersection energies are referred to the ground state minimum.

	target	semiemp.	weight
at S_0 minimum			
$\Delta E(S_1 - S_0)$	3.36	2.85	1.0
$\Delta E(S_2 - S_0)$	4.05	3.58	1.5
$\Delta E(T_1 - S_0)$	3.10	2.63	1.0
$\Delta E(T_2 - S_0)$	3.31	2.78	1.0
$\Delta E(T_3 - S_0)$	4.24	2.82	1.0
S_0-S_1 osc. strength	0.00	0.00	1.0
S_0-S_2 osc. strength	0.53	0.37	1.0
T_1-T_2 osc. strength	0.00	0.00	1.0
$\Delta E(S_1 - S_0)$, adiabatic	3.14	2.50	0.1
at S_1 minimum			
$\Delta E(S_1 - S_0)$	2.06	1.95	1.0
$\Delta E(S_2 - S_0)$	3.06	3.10	1.0
$\Delta E(T_1 - S_0)$	2.01	1.88	1.0
$\Delta E(T_2 - S_0)$	2.05	2.12	1.0
at S_2 minimum/ at $(S_2(\pi\pi^*_{CS})/S_1(n\pi^*_{CS})_{CI})$			
$\Delta E(S_1 - S_0)$	2.23	2.46	1.0
$\Delta E(S_2 - S_0)$	2.33	2.46	1.0
$\Delta E(T_1 - S_0)$	2.16	1.97	1.0
$\Delta E(T_2 - S_0)$	2.51	2.27	1.0
at T_1 minimum			
$\Delta E(S_1 - S_0)$	2.29	2.83	1.0
$\Delta E(S_2 - S_0)$	3.02	3.06	1.0
$\Delta E(T_1 - S_0)$	2.14	1.70	1.0
$\Delta E(T_2 - S_0)$	2.18	2.37	1.0
at T_2 minimum			
$\Delta E(S_1 - S_0)$	2.52	2.20	1.0
$\Delta E(S_2 - S_0)$	2.66	3.14	1.0
$\Delta E(T_1 - S_0)$	1.96	2.11	1.0
$\Delta E(T_2 - S_0)$	2.68	2.11	1.0
at $(S_1 (\pi\pi^*_{CC})/S_0)_{CI}$			
$E(S_1 (\pi\pi^*_{CC})/S_0)$, adiabatic	3.90	2.97	2.0
at $(S_1 (\pi\pi^*_{CS})/S_0)_{CI}$			
$E(S_1 (\pi\pi^*_{CS})/S_0)$, adiabatic	3.82	3.38	2.0

Table S4. Reparameterization of the AM1 Hamiltonian: target values for internal coordinates, and corresponding semiempirical results. Distances in angstroms, angles in degrees.

	target	semiemp.	weight		target	semiemp.	weight
at S_0 minimum				*at S_2 minimum*			
∠$SC_9C_3C_4$	179.5	171.1	0.5	∠$SC_9C_3C_4$	-173.8	-174.5	0.0
∠$C_9N_8C_7N_6$	0.5	1.8	0.5	∠$C_9N_8C_7N_6$	6.8	-0.7	0.5
∠SC_9N_8	121.1	115.6	0.5	∠SC_9N_8	115.3	121.0	0.5
∠SC_9C_3	129.4	129.8	0.5	∠SC_9C_3	126.7	120.2	0.5
R_{SC}	1.64	1.6	0.5	R_{SC}	1.75	1.69	0.5
∠$N_8C_7N_{10}H$	-40.2	-52.3	0.5	∠$N_8C_7N_{10}H$	-148.7	-124.2	1.2
∠$N_8C_7N_{10}$	115.7	116.4	0.5	∠$N_8C_7N_{10}$	113.1	113.4	0.5
∠$N_8C_7N_6$	124.2	125.5	0.5	∠$N_8C_7N_6$	118.3	124.7	0.5
at S_1 minimum				*at T_1 minimum*			
∠$SC_9C_3C_4$	148.9	158.9	2.0	∠$SC_9C_3C_4$	149.0	150.2	1.5
∠$C_9N_8C_7N_6$	7.5	11.3	0.5	∠$C_9N_8C_7N_6$	5.9	0.7	0.5
∠SC_9N_8	115.1	116.8	0.5	∠SC_9N_8	115.4	118.4	0.5
∠SC_9C_3	122.0	121.3	0.5	∠SC_9C_3	122.3	125.7	0.5
R_{SC}	1.78	1.69	0.5	R_{SC}	1.79	1.60	0.5
∠$N_8C_7N_{10}H$	-47.3	-55.2	0.5	∠$N_8C_7N_{10}$	114.9	119	0.5
∠$N_8C_7N_{10}$	113.2	113.4	0.5	∠$N_8C_7N_6$	124.8	123.8	0.5
∠$N_8C_7N_6$	125.9	127.8	0.5	*at T_2 minimum*			
at (S_1 ($\pi\pi^*_{CC}$)/S_0)$_{CI}$				∠$SC_9C_3C_4$	148.9	138.2	1.5
∠$SC_9C_3C_4$	176.3	178.4	1.5	∠$C_9N_8C_7N_6$	-6.2	-2.4	0.5
∠$C_9N_8C_7N_6$	-62.5	-66.1	0.5	∠SC_9N_8	122	116.1	0.5
∠SC_9N_8	120.5	118.8	0.5	∠SC_9C_3	124.7	121.8	0.5
∠SC_9C_3	127	127.2	0.5	R_{SC}	1.79	1.69	0.5
R_{SC}	1.64	1.60	0.5	∠$N_8C_7N_{10}$	111.6	113.3	0.5
∠$N_8C_7N_{10}$	117.9	114.2	0.5	∠$N_8C_7N_6$	117.4	126.7	0.5
∠$N_8C_7N_6$	112.6	114.2	0.5				
at (S_1 ($\pi\pi^*_{CS}$)/S_0)$_{CI}$							
∠$SC_9C_3C_4$	96.1	-101	1.5				
∠$C_9N_8C_7N_6$	20.2	32.4	0.5				
R_{SC}	1.82	1.66	0.5				

Table S5. Semiempirical parameters used in this work (AM1 Hamiltonian).

	units	C	H	N	S
U_{ss}	eV	-51.70567442	-11.96067697	-70.73190877	-54.99016001
U_{pp}	eV	-39.01431556		-57.48965377	-48.17438782
β_s	eV	-16.58114161	-5.76544469	-20.69281460	-1.93289372
β_p	eV	-8.14284151		-15.85836765	-8.66729059
ζ_s	bohr^{-1}	1.87028423	1.08267366	2.39578698	2.15529727
ζ_p	bohr^{-1}	1.77544336		1.98653295	1.89843699
g_{ss}	eV	13.07843585	13.98321296	13.11440461	12.65129973
g_{sp}	eV	11.39161263		13.18340832	8.65807813
g_{pp}	eV	11.06204170		13.83589967	8.64416794
g_{p2}	eV	9.49361026		12.07993686	7.76551987
h_{sp}	eV	1.57354148		5.03549967	3.92958663
α	Å^{-1}	2.79987197	3.06835947	2.97019267	2.44690414
K_1		0.07462271	0.10288875	0.06073380	-0.74601055
L_1	Å^{-1}	5.73921605	5.90172268	4.58892946	4.81038002
M_1	Å	1.04396983	1.17501185	1.37873881	0.59380129
K_2		0.01177053	0.06457449	0.02438558	-0.06519286
L_2	Å^{-1}	6.92401726	6.41785671	4.62730519	7.20760864
M_2	Å	1.66159571	1.93844484	2.08370698	1.29492008
K_3		0.03720662	-0.03567387	-0.02283430	-0.00655977
L_3	Å^{-1}	6.26158944	2.80473127	2.05274659	9.00000180
M_3	Å	1.63158721	1.63655241	1.86763816	1.80060151
K_4		-0.00270657			
L_4	Å^{-1}	9.00003735			
M_4	Å	2.79557901			

The parameters P_1 and P_2 used in the added potential $U(\theta, \phi)$ defined in equation 2 of the main text are, in eV:
$P_1 = -0.5233379537$ and $P_2 = 0.767766833$.